

A fully dispersive fifth order nonlinear wave model.II: Numerical simulation

^aY. ZHANG & W.B. FENG, ^bX.Q. JI, ^cM.M. WANG

^aCollege of Harbour, Coastal and Offshore Engineering, Hohai University, Nanjing, Jiangsu, P.R.C

^bJiangsu Provincial Water Transport Engineering Technique Research Center, Nanjing, P.R.C

^cJiangsu Province Engineering Consulting Center, Nanjing, P.R.C

KEYWORD: Nonlinear waves; Numerical solution; Water waves; Nonlinear model; Dispersion

ABSTRACT: This paper presents the numerical solution of a fully dispersive fifth order nonlinear wave propagation model. The new equations are directly applicable to the wave propagation from deep water to shallow water and solved numerically with a finite difference method. A moving grid in spatial difference and a “homeomorphic linear Prediction-Correction-Iteration” Crank-Nicolson method was used to discretize the models. The numerical models are applied to an elliptic shoal (reported by Berkhoff et al. (1982)) and a submerged breakwater (reported by Ohyama et al. (1995)). Comparison of the results shows that the present models predict the measurements well, can be used to depict wave propagation for deep water to shallow water, across obstacles.

INTRODUCTION

In coastal engineering, two types of equations are widely accepted for the simulation of combined refraction-diffraction of water waves, one is the mild-slope equation by Berkhoff (1972) et al; the other is the Boussinesq equations by Peregrine (1967) et al. In spite of their popularity, both equations have limitations. To breakthrough this limitations, Nadaoka (1994), Isobe (1994), Li Bin (2008) and Hong (2009) et al proposed the mathematical models which satisfied fully dispersion and nonlinearity simultaneously by adopting different factors.

A second order mathematical model was established by Hong *et al* (2009). To suppress high frequency wave, a new algorithm named “homeomorphic linear prediction-correction-iteration” method was established. Low order terms were divided from the high order terms. Prediction and correction steps were carried out in time difference for low order equations. The calculation results were as initials for high order equations and the whole iteration process was carried out until accuracy requirements satisfied. Wu (2009) validated the model thoroughly. Zhang (2010) improved the second order model and extended the mathematical model to third order. A unified model was established. By changing coefficients, the lower model (linear, second order, third order) could easily unified and separated. A systematic validation of this third order model and its lower modes were carried out. The results indicate that the higher order model fits well for wave propagating from deep water to shallow water. In this paper, a fully dispersive fifth order nonlinear wave propagation model will be solved and validated.

GOVERNING EQUATIONS

The fully dispersive fifth order nonlinear wave propagation model (current=0) for slowly varied topography can be written in a unified form as follows:

$$\frac{\partial h}{\partial t} = -\frac{1}{A} \left[A_3 \left(\frac{\partial^2 \Phi}{\partial^2 x} + \frac{\partial^2 \Phi}{\partial^2 y} \right) + \left(\frac{\partial A_3}{\partial x} \frac{\partial \Phi}{\partial x} + \frac{\partial A_3}{\partial y} \frac{\partial \Phi}{\partial y} \right) \right] + A_4 \Phi = E(h, \Phi) \quad (1)$$

$$\begin{aligned} \frac{\partial \Phi}{\partial t} = & -\frac{1}{B_1} \{ gh + [B_4(\frac{\partial \Phi}{\partial x} + \frac{\partial \Phi}{\partial y}) + \frac{\partial B_1}{\partial t} + W B_1] \Phi \\ & + \frac{B_2}{2} [(\frac{\partial \Phi}{\partial x})^2 + (\frac{\partial \Phi}{\partial y})^2] + \frac{B_3}{2} \Phi^2 \} = F(h, \Phi) \end{aligned} \quad (2)$$

the coefficients are:

$$\begin{aligned} A_1 = B_1 = & 1 + \frac{s^2}{g} h + \frac{1}{2} (kh)^2 + \frac{1}{6} \frac{s^2}{g} k^2 h^3 \\ & + \frac{1}{3} \frac{s^2}{g} k^2 h^4 + \frac{1}{24} (kh)^4 \end{aligned} \quad (3)$$

$$A_3 = \frac{\epsilon \epsilon_g}{g} + h + \frac{s^2}{g} h^2 + \frac{1}{3} [k^2 + (\frac{s^2}{g})^2] h^3 \quad (4)$$

$$\begin{aligned} A_4 = & \frac{k^2 \epsilon \epsilon_g}{g} + \frac{J}{g} - \frac{s^2}{g} [1 + \frac{s^2}{g} h + (kh)^2 + \frac{1}{3} (kh)^4] \\ & - \frac{1}{3} [k^2 + (\frac{s^2}{g})^2] k^2 h^3 \end{aligned} \quad (5)$$

$$B_2 = 1 + 2 \frac{s^2}{g} h + [k^2 + (\frac{s^2}{g})^2] h^2 + \frac{4}{3} \frac{s^2}{g} k^2 h^3 \quad (6)$$

$$\begin{aligned} B_3 = & (\frac{s^2}{g})^2 + 2 \frac{s^2}{g} k^2 h + [k^2 + (\frac{s^2}{g})^2] (kh)^2 \\ & + \frac{4}{3} \frac{s^2}{g} k^4 h^3 \end{aligned} \quad (7)$$

$$B_4 = \nabla \frac{s^2}{g} h + \frac{1}{2} h^2 \nabla [k^2 + (\frac{s^2}{g})^2] \frac{s^2}{g} \nabla h \quad (8)$$

where η is wave surface elevation; Φ is velocity potential function; x, y are horizontal directions; t is time variable; J is topography coefficient; s is angular frequency considering diffraction effect; k is wave number; ϵ is wave celerity; ϵ_g is group velocity; $\nabla \equiv (\partial/\partial x, \partial/\partial y)$ is horizontal gradient operator.

Omitting the high order terms, the lower order linear model could be obtained.

$$\begin{aligned} \frac{\partial h}{\partial t} = & -[\frac{\epsilon \epsilon_g}{g} \nabla \cdot \nabla \Phi + \nabla \frac{\epsilon \epsilon_g}{g} \cdot \nabla \Phi] + \frac{1}{g} (k \epsilon \epsilon_g + J - s^2) \Phi \\ = & E(h, \Phi) \end{aligned} \quad (9)$$

$$\frac{\partial \Phi}{\partial t} = -(gh + W \Phi) = F(h, \Phi) \quad (10)$$

NUMERICAL METHOD

Using front difference in time step and central difference varied moving grid in space step to solve the governing equations. $\Delta x, \Delta y$ are space steps and Δt is time step. The improved Crank-Nicholson Prediction-Correction-Iteration method was adopted. This algorithm is stable unconditionally.

Spatial Difference

The derivation of first order and second order for moving grid are as follows:

$$\left(\frac{\partial\Phi}{\partial x}\right)_{i,j}^n = \frac{\Phi_{i+1,j}^n - \Phi_{i-1,j}^n}{x_{i+1,j} - x_{i-1,j}} ; \left(\frac{\partial\Phi}{\partial y}\right)_{i,j}^n = \frac{\Phi_{i,j+1}^n - \Phi_{i,j-1}^n}{x_{i,j+1} - x_{i,j-1}} \quad (11)$$

$$\begin{aligned} \left(\frac{\partial^2\Phi}{\partial x^2}\right)_{i,j}^n &= \frac{\Phi_{i-1,j}^n}{(x_{i,j} - x_{i-1,j})(x_{i+1,j} - x_{i-1,j})} \\ &- \frac{2\Phi_{i,j}^n}{(x_{i,j} - x_{i-1,j})(x_{i+1,j} - x_{i,j})} \quad (12) \\ &+ \frac{\Phi_{i+1,j}^n}{(x_{i+1,j} - x_{i-1,j})(x_{i+1,j} - x_{i,j})} \end{aligned}$$

$$\begin{aligned} \left(\frac{\partial^2\Phi}{\partial y^2}\right)_{i,j}^n &= \frac{\Phi_{i,j-1}^n}{(x_{i,j} - x_{i,j-1})(x_{i,j+1} - x_{i,j-1})} \\ &- \frac{2\Phi_{i,j}^n}{(x_{i,j} - x_{i,j-1})(x_{i,j+1} - x_{i,j})} \quad (13) \\ &+ \frac{\Phi_{i,j+1}^n}{(x_{i,j+1} - x_{i,j-1})(x_{i,j+1} - x_{i,j})} \end{aligned}$$

Mathematical Solution

Prediction step :

$$h_{i,j}^{n+\frac{1}{2}} = h_{i,j}^n + \frac{\Delta t}{2} E_{i,j}^n ; \Phi_{i,j}^{n+\frac{1}{2}} = \Phi_{i,j}^n + \frac{\Delta t}{2} F_{i,j}^n \quad (14)$$

Correction step :

$$h_{i,j}^{n+1} = h_{i,j}^{n+\frac{1}{2}} + \frac{\Delta t}{2} E_{i,j}^{n+\frac{1}{2}} ; \Phi_{i,j}^{n+1} = \Phi_{i,j}^{n+\frac{1}{2}} + \frac{\Delta t}{2} F_{i,j}^{n+\frac{1}{2}} \quad (15)$$

Iteration step :

$$\begin{aligned} h_{i,j}^{n+1} &= h_{i,j}^n + \Delta t [bE_{i,j}^{n+1} + (1-b)E_{i,j}^n] \\ \Phi_{i,j}^{n+1} &= \Phi_{i,j}^n + \Delta t [bF_{i,j}^{n+1} + (1-b)F_{i,j}^n] \end{aligned} \quad (16)$$

where β is relaxation factor, $0 \leq \beta \leq 1$, here $\beta=0.5$.

Numerical Process

The “homeomorphic linear prediction-correction-iteration” method was adopted here to solve the governing equations. The procedure is as follows:

1) Preparation Step: Divide the governing equation by linear terms and nonlinear terms; set time step Δt and space step Δx , Δy (moving grid or homogenous grid); set water depth of grids; set the boundary condition, initial condition and other parameters; set initials for the whole water area;

2) Prediction step: calculate the linear velocity potential and wave surface elevation of all grids at time $n+1/2$;

3) Correction step: by using the linear velocity potential and wave surface elevation of all grids at time $n+1/2$, Calculate the values of velocity potential and wave surface elevation of all grids at time $n+1$;

4) Iteration step: taking the calculation results of the correction step as initials, adopt the nonlinear governing equations and iterate until the accuracy satisfies.

5) Propagation step: take the results of the iteration step as initials and repeat step2)-4) until the end of the whole time steps.

Boundary conditions

Incident boundary condition

The Φ and η at incident boundary could be given by the following equations.

$$\Phi(x_0, y, t) = -\frac{ig}{w} a_0 e^{i(k_0 x_0 \cos q_0 + k_0 y \sin q_0 - wt)} \quad (17)$$

$$h(x_0, y, t) = a_0 e^{i(k_0 x_0 \cos q_0 + k_0 y \sin q_0 - wt)} \quad (18)$$

where X_0 is incident boundary location; i is imaginary part; k_0 is wave number; q_0 is the incident wave angle to x axis; ω is angular frequency.

The reflection wave will grow in calculation domain. When propagating into the incident boundary, the reflection wave will interact with the incident wave and makes the incident condition changed. This will make the final calculation results distorted. A simple method to solve this problem is increasing the incident distance. This method is efficient. But calculation time was greatly enlarged. Here a Tanimot-type boundary condition was set to eliminate reflection waves. The incident boundary conditions could be rewritten as:

$$\Phi(x_0, y, t) = \Phi_l(x_0, y, t) + \Phi_R(x_0, y, t) \quad (19)$$

$$h(x_0, y, t) = h_l(x_0, y, t) + h_R(x_0, y, t) \quad (20)$$

where

$$\Phi_R(x_0, y, t) = \Phi_l(x_0 + \Delta x, y, t - t) - \Phi_l(x_0 + \Delta x, y, t - t) \quad (21)$$

$$h_R(x_0, y, t) = h_l(x_0 + \Delta x, y, t - t) - h_l(x_0 + \Delta x, y, t - t) \quad (22)$$

Φ, η are theoretical results of Eqs. (17), (18), Φ_l, h_l are calculation results of the model.

Outflow boundary condition

To eliminate the reflection wave better, the “time and space staggered unified boundary condition” by Hong (1999) and sponge layer were combined to deal with the outflow boundary condition. The expressions are as follow:

$$\Phi(x_n, y, t) = A\Phi(x_n - \Delta x, y, t - t) \quad (23)$$

where

$$A = \sqrt{\frac{1 + 2k_r \cos e_r + k_r^2}{1 + 2k_r \cos(k_x \Delta x + e_r) + k_r^2}} \quad (24)$$

t can be calculated by the following equation

$$\tan(wt) = \frac{(k_r^2 - 1) \sin(k_x \Delta x)}{\cos(k_x \Delta x) + k_r \cos(k_x \Delta x + e_r)} \quad (25)$$

where k_r, ε_r are reflection coefficient and reflection phase difference, $k_r=0$ is open boundary condition and $0 < k_r \leq 1$ are reflection boundary condition. A sponge layer was also adopted here. The elimination effect was mainly determined by friction coefficient μ .

MODEL VALIDATION

Wave propagating over an elliptic shoal

To test the new parabolic model, propagation of simple harmonic linear waves over an elliptic shoal, which was reported by Berkhoff *et al.* (1982) is first considered. Berkhoff *et al.* (1982) carried out a physical model test on the topography that an elliptic shoal was set on a uniform slope. And measured data at 8 sections was obtained. Figure 1. shows the topography.

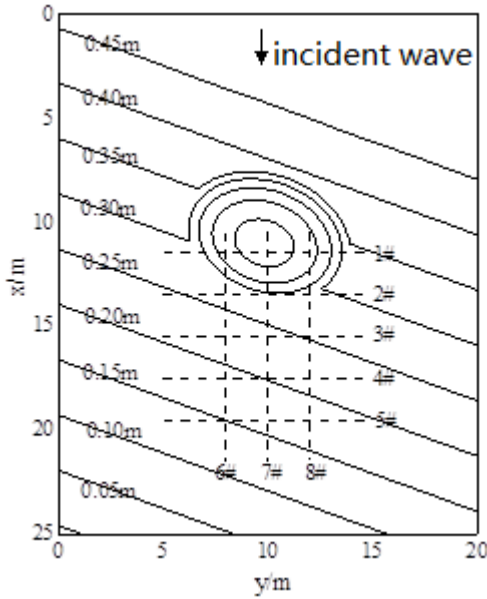


Figure 1. Topography of elliptic shoal and measurement transects

$$\begin{cases} x' = (x - 10.5) \cos 20^\circ - (y - 10) \sin 20^\circ \\ y' = (x - 10.5) \sin 20^\circ + (y - 10) \cos 20^\circ \end{cases} \quad (26)$$

The center coordinates of elliptic shoal is $(x', y') = (0, 0)$ and the boundary condition is $(x'/3)^2 + (y'/4)^2 = 1$.

The depth at the flat area and the uniform slope are:

$$h_s = \begin{cases} 0.45 & x' < -5.82 \\ 0.45 - 0.02(5.82 + x') & x' \geq -5.85 \end{cases} \quad (27)$$

The depth at the elliptic shoal could be:

$$h = h_s - 0.5 \left[1 - \left(\frac{x'}{3.75} \right)^2 - \left(\frac{y'}{5} \right)^2 \right]^{1/2} + 0.3 \quad (28)$$

The incident wave height is 0.0464m and period is 1.0s. $\Delta x = \Delta y = 0.1m, \Delta t = 0.1s$. The relative wave height of the nonlinear wave model and measured data at the 8 sections were shown in Figure2. The result indicated that the nonlinear model fits the measured data well, and the high order model is effective.

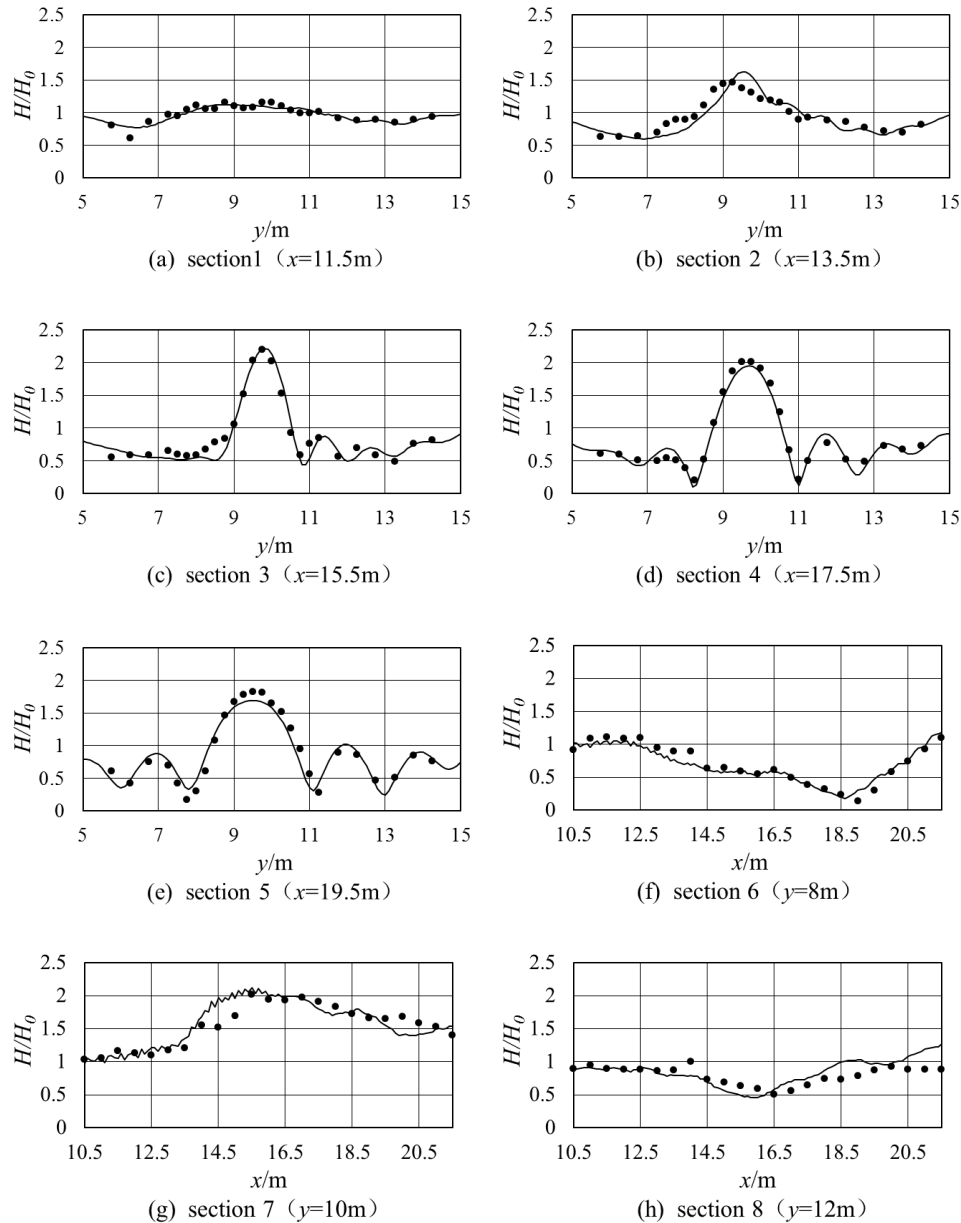


Figure 2. Comparison among numerical results and experimental data for the elliptic shoal (\cdot —measured data, —numerical result)

Submerged breakwater validation

When wave propagates over submerged breakwaters in shallow water, main wave energy would rapidly change from low frequency to high frequency due to nonlinearity. The phase difference between the high frequency boundary and the free surface would cause harmonic source vibration, i.e. the related wave. For the long main wave, the dispersion of free high frequency harmonic waves is the main factor to wave deformation. Wave energy transferred between harmonic waves when wave propagate over submerged breakwaters, each high frequency wave transmitted in its own phase velocity, the wave form changed rapidly. The relative wave number kh (k is wave number, h is water depth) at deep water is larger than that at submerged breakwater crest. This required the mathematical model has good applicability in high frequency wave domain.

Measured Data

Ohyama *et al*(1995) adopted the following flume to study wave propagation on submerged breakwater to test the nonlinear wave model. The flume is 65m in length, 1.0m in width, and 1.6m in height. The center of submerged breakwater is 28.3m away from wavemaker and the wave damping me-

chanics was set on the other side. The water depth is 0.5m at bottom and 0.15m at crest. Figure 3. gives the layout and stations of Ohyama test.

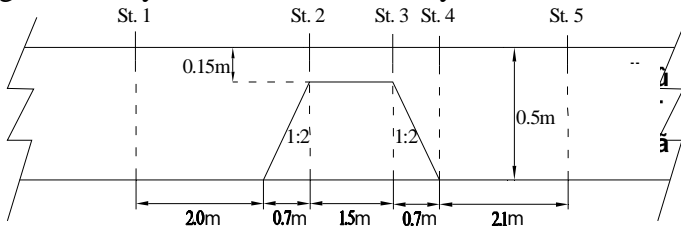


Figure 3. Layout and stations of submerged breakwater (Ohyama,1995)

Model Results and Discussion

Four set incident wave elements were chosen to test this numerical model (Table 1). T is wave period, H is wave height, k_0 and k_s can be determined by linear dispersion relationship of small amplitude wave, Ur is Ursell number($=gHT^2/h^2$), reflecting the degree of nonlinearity, the subscript “0” and “s” represents the location of deep water ($h_0=0.5m$) and the crest ($h_s=0.15m$).

Since the topography changed rapidly at submerged breakwater, small space step may cause divergence and the large space step may neglect the important information of propagation. The “Moving grid method” were adopted here to adjust space step to get a more realistic result. Δx_1 is space step at deep water and Δx_2 is at crest. For case 1~3, $\Delta x_1=L_0/30$, $\Delta x_2=L_0/32$, $\Delta t=T/32$. For case4, $\Delta x_1=L_0/40$, $\Delta x_2=L_0/60$, $\Delta t=T/64$.

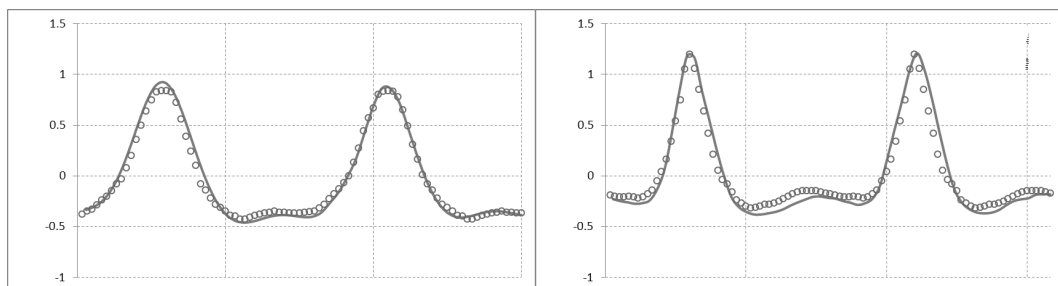
The results of Station3 and Station5 were compared with the measured data.

Table 1. Incident wave elements of Ohyama model test

Cases	Period $\frac{T}{(s)}$	Relative wave heigh H/h_0	k_0h_0	$kshs$	$(Ur)_0$	$(Ur)_s$
case1	1.34	0.05	1.299	0.614	1.8	21.6
case2	1.34	0.1	1.299	0.614	3.5	43.3
case3	2.01	0.1	0.769	0.396	7.9	108.7
Case4	2.68	0.1	0.555	0.294	14.1	201.5

Results in shallow water area

Comparison of numerical results and measured data at Station3 were shown in Figure 4. The vertical axis is the ratio of wave surface elevation to incident wave height, i.e. η/H_0 and the horizontal axis stands for time process. Station3 is at the crest of submerged breakwater. The water depth is relatively small. The accuracy of result depends on the degree of nonlinearity of the test model. Generally speaking, the model result fits well with the measured data. The incident wave is short wave in case1 and the nonlinearity is weak, the results show high accuracy. As the degree of nonlinearity goes higher, the result is less idealistic. It indicates that as the nonlinearity goes higher, errors may goes larger for the 5th order model.



(a) Case 1 $H=0.025m$, $T=1.34s$

(b) Case 2 $H=0.05m$, $T=1.34s$

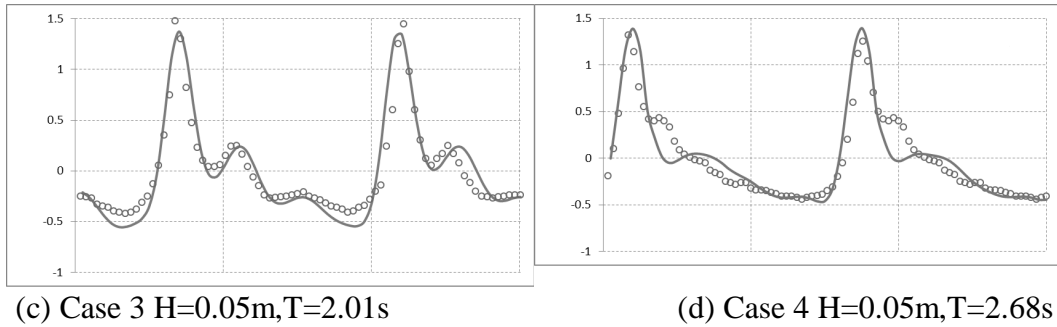


Figure 4. Comparison of Numerical results and measured data at Station3 (t'/T0 for x axis and η/H₀ for y axis; oexperimental data;-numerical result)

Results after submerged breakwater

Comparison of numerical results and measured data at Station5 were shown in Figure 5. The vertical axis is η/H₀ and the horizontal axis stands for time process t/T₀. The high frequency harmonic waves occur when wave propagating over the crest of submerged breakwater and they propagate in the form of free wave at the back area of submerged breakwater. Seen from Figure 5, wave deformation is strong when wave propagate over the submerged breakwater and the wave shape is not symmetry and the related wave occurs. The result is consistent with the measured data. This indicated that the calculation result is dependable. It can be used to simulate the wave transmitted after submerged breakwaters.

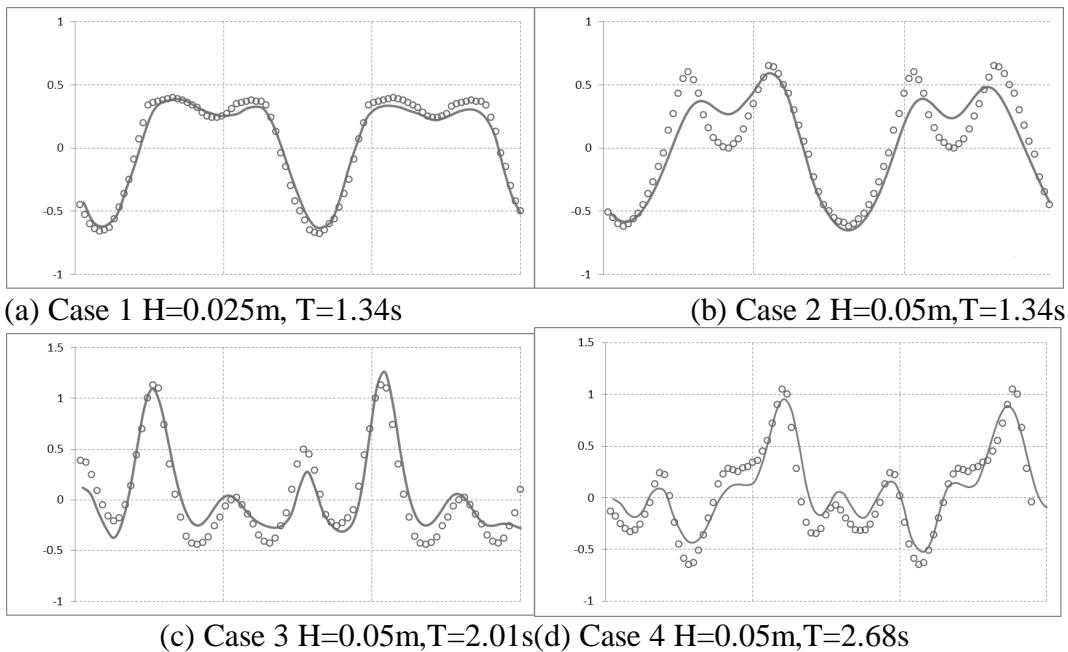


Figure 5. Comparison of Numerical results and measured data at Station5 (t'/T0 for x axis and η/H₀ for y axis; o experimental data; -numerical result)

CONCLUSIONS

- 1) A numerical algorithm of fully dispersive fifth order nonlinear wave propagation model for mild current, water level and depth was established in this paper.
- 2) A moving grid in spatial difference and a “homeomorphic linear Prediction-Correction-Iteration” Crank-Nicolson method was used to discretize the models.
- 3) The numerical models are applied to an elliptic shoal (reported by Berkhoff *et al.* (1982)) and a submerged breakwater (reported by Ohyama *et al.* (1995)). Comparison of the results shows

that the present models generally predict the measurements well, can be used to depict waved propagation for deep water to shallow water, across obstacles.

ACKNOWLEDGEMENT

The authors wish to acknowledge the support of the National Science Foundation of China (Grant No. 51279055; 51579090) and the Fundamental Research Funds for Central Universities (2011B06114).

REFERENCE

- 1) Berkhoff, J.C.W., 1972. Computation of combined refraction-diffraction. In: *Proc. 13th Int. Conf. Coastal Eng., Vancouver*. ASCE, pp. 471-490.
- 2) Hong, G.W., & Zhang H.S. 1999. Nonlinear wave simulation on varied water depth[J]. *ocean engineering*, Vol.17, No.4: 64~73(in Chinese).
- 3) Hong G.W., Wu Z. & Zhang Y. 2009. Nonlinear mathematical model for Gravity wave propagation on the long wave.[C]. *The 14th National Symposium on Coastal Engineering* , 2009:21~34.
- 4) Isobe, M. 1994. Time-dependent mild slope equation for random waves. [C]. Japan: *Proceeding of the 24th International Conference on Coastal Engineering*:285-299.
- 5) Li. B., 2008. Wave equations for regular and irregular water wave propagation. [J]. *Journal of waterway, port, coastal and ocean engineering*, 134(2):121~142.
- 6) Nadaoka, K, Beji, S & Nakagawa, Y. A., 1994. fully-dispersive nonlinear wave model and its numerical solutions. [C]. Japan: *Proceedings of the 24th International Conference on Coastal Engineering*:427~441.
- 7) Ohyama, T., Kioka, W., & Tada, A., 1995. Application of numerical models to nonlinear dispersive wave[J]. *Cosatal Engineering*.,24:297-313.
- 8) Peregrine, D.H., 1967. Long waves on a beach. *J. Fluid Mech.*, 27: 815-827.
- 9) Wu., Z., 2009. Fully dispersion nonlinear wave propagation model and its simulation[C]. *The 14th National Symposium on Coastal Engineering* , 2009:448~457.
- 10) Zhang Y. 2010. Fully dispersion nonlinear mathematical wave propagation model and its simulation[D]. Nanjing: Hohai University , 2010